Muon $g-2$ in the 2HDM: Maximum results and detailed phenomenology

Adriano Cherchiglia,[1] Dominik Stöckinger,[2] and Hyejung Stöckinger-Kim[2]

[1]*Universidade Federal do ABC - Centro de Ciências Naturais e Humanas, Santo André 09210-580, Brazil*

[2]*Institut für Kern- und Teilchenphysik, TU Dresden, 01069 Dresden, Germany*

(Received 8 April 2018; published 1 August 2018)

We analyze the maximum contributions to the muon magnetic moment a_μ and Yukawa and triple Higgs couplings in the flavor-aligned two-Higgs doublet model (2HDM). We focus on the most promising case of a light pseudoscalar Higgs A with large Yukawa couplings to leptons and quarks. Taking into account experimental constraints from LHC Higgs and flavor physics, we find maximum possible Yukawa couplings of a light A of around 50–100 (leptons) and $\mathcal{O}(0.5)$ (quarks). An overall maximum of a_μ of more than 45×10^{-10} is possible in a very small parameter region around $M_A = 20$ GeV. For M_A up to 100 GeV, the maximum possible value of a_μ is compatible with the currently observed deviation if the A couplings to quarks and leptons are both large, making this scenario promising for LHC searches. We also analyze the subleading bosonic two-loop contributions to a_μ, finding values up to 3×10^{-10}.

DOI: 10.1103/PhysRevD.98.035001

I. INTRODUCTION

The two-Higgs doublet model (2HDM) is one of the most common extensions of the Standard Model (SM). It is the simplest model with nonminimal electroweak symmetry breaking, comprising two SU(2) doublets and five physical Higgs bosons h, H, A, and $H^\pm$, where h must be SM-like to agree with LHC data. The extra Higgs bosons are actively searched for at the LHC.

For more than a decade the measured value [1] of the anomalous magnetic moment of the muon $a_\mu = (g-2)_\mu/2$ has shown a persisting deviation from the current SM prediction [for recent developments see Refs. [2–5] (QED and electroweak corrections) and [6–19] (QCD corrections)]. Using the evaluation of the indicated references, the current deviation is

$$a_\mu^{\mathrm{Exp-SM}} = \begin{cases} (26.8 \pm 7.6) \times 10^{-10} \text{ [6]}, \\ (28.1 \pm 7.3) \times 10^{-10} \text{ [9]}, \\ (31.3 \pm 7.7) \times 10^{-10} \text{ [10]}. \end{cases} \qquad (1)$$

a_μ provides a tantalizing hint for new physics. The hint might be strongly sharpened by a new generation of a_μ measurements at Fermilab and J-PARC [20,21]. Hence it is of high interest to identify new physics models which are able to explain the current deviation, or a future larger or smaller deviation.

Recently it has been repeatedly stressed that the 2HDM is such a model. This is a nontrivial observation since the leading 2HDM contributions to a_μ arise only at the two-loop level and small Higgs masses are needed to compensate the two-loop suppression. Specifically, the authors of Refs. [22–27] studied the so-called type X (or lepton-specific) model, and the authors of Refs. [28–30] the more general (flavor-)aligned model [31,32]. In all these cases it was shown that a light pseudoscalar A boson with large couplings to leptons is viable and could explain Eq. (1) or at least most of it. The authors of Ref. [28] also found an additional small parameter region with very light scalar H; furthermore, the authors of Ref. [33] studied a Z_4-symmetric, "muon-specific" model which can explain Eq. (1) for $\tan\beta \sim 1000$.

At the same time, the accuracy of the a_μ prediction in the 2HDM has increased. The authors of Ref. [30] computed the 2HDM contributions fully at the two-loop level, including all bosonic contributions (from Feynman diagrams without closed fermion loop). Prior to that, the author of Ref. [29] computed all contributions of the Barr-Zee type [34]. As a result of these calculations, the 2HDM theory uncertainty is fully under control and significantly below the theory uncertainty of the SM prediction and the resolution of the future a_μ measurements.

Here we employ the full two-loop prediction to carry out a detailed phenomenological study of a_μ in the general flavor-aligned 2HDM and of the parameters relevant for a_μ. In detail, the questions we consider are

(i) What are the constraints on the 2HDM parameters most relevant for a_μ (the mass of the A boson and its Yukawa couplings to leptons and quarks, and further 2HDM masses and Higgs potential parameters)?

(ii) In which parameter region can the 2HDM accommodate the current deviation in a_μ (or a future, possibly larger or smaller deviation)?

(iii) What is the overall maximum possible value of a_μ that can be obtained in the 2HDM (for various choices of restrictions on the Yukawa couplings)?

We will generally focus on the promising scenario with $M_A < M_h$ and allow for general flavor-aligned Yukawa couplings but will comment also on the more restrictive case of the lepton-specific type X model. We will take into account constraints from theoretical considerations such as tree-level unitarity and perturbativity, experimental constraints from collider data from LHC and LEP, and constraints from B- and τ-physics.

The outline of the paper is as follows. In Sec. II, we describe our setup and give details on the definition of the 2HDM. Section III then discusses the detailed constraints on the parameters most relevant for a_μ in the 2HDM: on the Higgs masses, on the Yukawa couplings, and on Higgs potential parameters and Higgs self-couplings. Section IV gives an updated discussion of the full bosonic two-loop contributions, taking into account detailed constraints on the parameters. Section V finally gives the results on a_μ in the 2HDM. The results are presented both as contour plots in parameter planes and as plots showing the maximum possible values of a_μ in the 2HDM.

II. SETUP

In this section we provide the basic relations for the two-Higgs doublet model and describe our technical setup.

A. Definition of the 2HDM

We use the 2HDM with general Higgs potential in the notation of Refs. [35,36]:

$$\begin{aligned} V(\phi_1,\phi_2) &= m_{11}^2\phi_1^\dagger\phi_1 + m_{22}^2\phi_2^\dagger\phi_2 - \{m_{12}^2\phi_1^\dagger\phi_2 + \text{H.c.}\} \\ &\quad + \frac{\lambda_1}{2}(\phi_1^\dagger\phi_1)^2 + \frac{\lambda_2}{2}(\phi_2^\dagger\phi_2)^2 + \lambda_3(\phi_1^\dagger\phi_1)(\phi_2^\dagger\phi_2) \\ &\quad + \lambda_4(\phi_1^\dagger\phi_2)(\phi_2^\dagger\phi_1) + \frac{1}{2}\{\lambda_5(\phi_1^\dagger\phi_2)^2 + \text{H.c.}\} \\ &\quad + \{[\lambda_6(\phi_1^\dagger\phi_1) + \lambda_7(\phi_2^\dagger\phi_2)]\phi_1^\dagger\phi_2 + \text{H.c.}\}. \end{aligned} \tag{2}$$

In the usual type I, II, X, and Y models a Z_2 symmetry is assumed which enforces that the two parameters λ_6 and λ_7 vanish. In the following we will investigate both the case with $\lambda_6 = \lambda_7 = 0$ and the case with nonvanishing λ_6, λ_7. Since we focus on the muon magnetic moment, which is not enhanced by CP violation, we assume all parameters to be real.[1] In the minimum of the potential the two-Higgs doublets acquire the vacuum expectation values (VEVs) $v_{1,2}$ with the ratio $\tan\beta = v_2/v_1$. It is then instructive to rotate the doublets by the angle β to the so-called Higgs basis [35–37], in which one doublet has the full SM-like VEV $v = \sqrt{v_1^2 + v_2^2}$ and the other doublet has zero VEV. The second doublet then contains the physical CP-odd Higgs A and the charged Higgs $H^\pm$, and the physical CP-even Higgs fields h, H correspond to mixtures between the two doublets in the Higgs basis with mixing angle $(\alpha - \beta)$. In practice we will choose the following set of independent input parameters:

$$M_{h,H,A,H^\pm}, \quad \tan\beta, \quad c_{\beta\alpha}, \quad \lambda_1, \quad \lambda_6, \quad \lambda_7, \tag{3}$$

where $c_{\beta\alpha} \equiv \cos(\beta - \alpha)$ and similar for $s_{\beta\alpha}$. We will further choose h to be the approximately SM-like Higgs state, which means that the mass M_h is fixed to the observed value of 125 GeV and that the mixing angle $c_{\beta\alpha}$ is small. It should be noted that all parameters in this list enter the prediction of the muon $g-2$ only at the two-loop level and hence do not have to be renormalized. We further note that the above parameter list is redundant, since it contains $\tan\beta$, which is unphysical in the fully general 2HDM. We use this parameter set since it allows a transparent comparison to the more restricted cases of the 2HDM with $\lambda_6 = \lambda_7 = 0$ and a Z_2 symmetry. The Appendix provides useful translation formulas between the generic basis and the Higgs basis.

For the Yukawa couplings we choose the setup of the (flavor-)aligned 2HDM of Ref. [31]. In this setup one assumes the following structure of the Yukawa couplings in the Higgs basis: the SM-like doublet has SM-like Yukawa couplings by construction; the other doublet has couplings proportional to the SM-like ones, with proportionality factors ζ_l (for charged leptons) and $\zeta_{u,d}$ (for up- and down-type quarks). For the mass-eigenstate Higgs bosons this implies the following Yukawa Lagrangian:

$$\begin{aligned} \mathcal{L}_Y = -\frac{\sqrt{2}}{v}H^+(\bar{u}[\zeta_d V_{\text{CKM}} M_d P_{\text{R}} - \zeta_u M_u V_{\text{CKM}} P_{\text{L}}]d \\ + \zeta_l \bar{\nu} M_l P_{\text{R}} l) - \sum_{\mathcal{S}=h,H,A}\sum_{f=u,d,l} \mathcal{S}\bar{f} y_f^{\mathcal{S}} P_{\text{R}} f + \text{H.c.}, \end{aligned} \tag{4}$$

where $P_{\text{R,L}} = \frac{1}{2}(1 \pm \gamma_5)$, and V_{CKM} is the Cabibbo-Kobayashi-Maskawa matrix. M_f denotes the diagonal 3×3 mass matrices. The Yukawa coupling matrices are defined as

$$y_f^{\mathcal{S}} = \frac{Y_f^{\mathcal{S}}}{v} M_f, \tag{5}$$

[1] See footnote 5 in Sec. VI.

TABLE I. Relation between the Yukawa parameters ζ_f in the general, aligned 2HDM and the usual type I, II, X, and Y models.

	Type I	Type II	Type X	Type Y
ζ_u	$\cot\beta$	$\cot\beta$	$\cot\beta$	$\cot\beta$
ζ_d	$\cot\beta$	$-\tan\beta$	$\cot\beta$	$-\tan\beta$
ζ_l	$\cot\beta$	$-\tan\beta$	$-\tan\beta$	$\cot\beta$

where

$$\begin{aligned} Y_f^h &= s_{\beta\alpha} + c_{\beta\alpha}\zeta_f, \\ Y_f^H &= c_{\beta\alpha} - s_{\beta\alpha}\zeta_f, \\ Y_{d,l}^A &= i\zeta_{d,l}, \\ Y_u^A &= -i\zeta_u. \end{aligned} \tag{6}$$

The flavor-aligned 2HDM contains the usual type I, II, X, and Y models as special cases; see Table I. Most notably, in type II, the product $|\zeta_u\zeta_d| = \cot\beta\tan\beta = 1$ is never small, implying very strong constraints from $b \to s\gamma$ for all values of $\tan\beta$ [38]. And in type X, $\zeta_l = -\tan\beta$ and $\zeta_u = \zeta_d = \cot\beta$ cannot be simultaneously large.

As shown in Refs. [32,39] the flavor-aligned scenario is minimal flavor violating and even though the alignment is not strictly protected by a symmetry, it is numerically rather stable under renormalization-group running. Hence we regard it as a theoretically and phenomenologically well-motivated and very general scenario.

B. Technical remarks

In order to check the viability of parameter points against experimental and theoretical constraints, we have adopted the routines implemented in the 2HDMC code [40], which allows checks regarding theoretical constraints such as stability, unitarity, and perturbativity of the quartic couplings; the S, T, and U precision electroweak parameters; and data from colliders implemented in the HiggsBounds and HiggsSignals packages [41,42].

For our later scans of parameter space we started with a wide range of all Higgs potential parameters in Eq. (3) and the Yukawa parameters $\zeta_{l,u,d}$. This range was narrowed down to

$$\begin{aligned} \zeta_d &= -0.7\text{–}1.1, & \lambda_1 &= 0\text{–}2\pi, \\ \lambda_6 &= -2\text{–}2, & \lambda_7 &= -3\text{–}3, \\ \tan\beta &= 0.3\text{–}2, & |c_{\beta\alpha}| &< 1/|\zeta_l|, \end{aligned} \tag{7}$$

after checking that this covers the parameter space with the largest possible contributions to all quantities of interest. Unless specified differently, these are the parameter ranges used in our scatter plots. In the plots evaluating a_μ, in addition we set $\zeta_d = 0$ to be specific, because this parameter has a very small influence on a_μ.

Regarding statistics, we have adopted the following procedure: first we constructed a χ^2 distribution for the physical process under consideration, and then we computed its respective p-value distribution, assuming that the errors are Gaussian and robust as usual [43]. Finally, we required that the p-value for the considered observable (or set of observables) be greater than 0.05 (corresponding to a 95% C.L. region). For the constraints to be discussed in Sec. III B, this approach is slightly different from the one implemented in Ref. [23], but we checked that the resulting exclusion contours are very similar.

III. CONSTRAINTS

In this section we provide a detailed investigation of experimental constraints on the 2HDM parameter space with general flavor-aligned Yukawa couplings. Earlier studies [22–30] and our later considerations show that a_μ can be promisingly large for small M_A and large ζ_l and ζ_u, so we focus on this scenario. Our study can be regarded as a generalization of Refs. [22,23,25], which focused on the lepton-specific (type X) case, where $\zeta_u = -1/\zeta_l = 1/\tan\beta$, and as complementary to Ref. [28], which focused on correlations in scans of parameter space. Our questions are as follows: What are the maximum values of ζ_l and ζ_u and other relevant parameters, and how do these maximum values depend on the value of the small Higgs mass M_A or the heavy Higgs masses?

We will begin with the most direct and basic constraints on the scenario with small M_A from collider physics, and then focus on maximum possible values of ζ_l and ζ_u and correlated parameters.

A. Basic collider constraints on small M_A and on mixing angle $\cos(\beta-\alpha)$

The scenario with light CP-odd Higgs boson A is obviously strongly constrained by collider physics. The most immediate constraints arise from negative results of direct A searches. On the one hand these results imply upper limits of the couplings between the A, W, and Z bosons and thus on the mixing angle $c_{\beta\alpha}$. However, below we will find much more severe limits on $c_{\beta\alpha}$, which are specific to our scenario with large ζ_l, so we will discuss only those in detail. On the other hand the negative searches for A imply upper limits on ζ_u in a restricted range of A masses; we will discuss these in Sec. III C.

In the remainder of this subsection we will discuss more interesting collider constraints on our scenario, which arise from measurements of the decays of the observed SM-like Higgs boson at the LHC. First, the LHC measurements of/searches for SM-like Higgs decays into τ pairs or muon pairs imply limits on the coupling of the SM-like Higgs boson to τ-leptons and muons. Expressed in terms of signal strengths, the recent Refs. [44,45] obtain

$$\mu_\tau = 1.09^{+0.27}_{-0.26}, \tag{8}$$

$$\mu_\mu = -0.1 \pm 1.4, \tag{9}$$

implying that the effective coupling of the SM-like Higgs to leptons Y_l^h in Eq. (6) cannot deviate strongly from unity and thus,[2]

$$|c_{\beta\alpha}\zeta_l| < \mathcal{O}(1). \tag{10}$$

The approximate form of this relation is sufficient for our purposes. The important points are that (*i*) for a given, large ζ_l, the mixing angle $c_{\beta\alpha}$ is strongly constrained particularly by the τ-coupling to be at most of the order of a percent, and (*ii*) the product $c_{\beta\alpha}\zeta_l$ cannot constitute an enhancement factor.

A second important implication of the SM-like Higgs decay measurements comes from the decay mode $h \to AA$, which is possible if $M_A < M_h/2$. A significant branching fraction for this decay is excluded by the agreement of the observed Higgs decays with the SM predictions. This implies strong constraints on the corresponding triple Higgs coupling C_{hAA}. It is therefore illuminating to analyze analytically the conditions for vanishing coupling C_{hAA}. Here we present useful approximations valid in the generic basis; the Appendix provides further details and formulas that are valid in the Higgs basis. We have to distinguish two cases:

(i) $M_A < M_h/2$ and large $\tan\beta$: In this limit, the requirement $C_{hAA} = 0$ reduces to

$$c_{\beta\alpha} = 2/\tan\beta + \mathcal{O}(1/\tan^2\beta). \tag{11}$$

For the type X model, where $\tan\beta = -\zeta_l$, Eq. (11) together with Eq. (6) implies $Y_l^h \approx -1$, the so-called wrong-sign muon Yukawa coupling, discussed recently in Ref. [27]. In the general case, this relation, together with the limit on $c_{\beta\alpha}$ from Eq. (10), implies a lower limit on $\tan\beta$, which is of the form $\tan\beta \gg |\zeta_l|$. This parameter region does not lead to distinctive phenomenology; we will not discuss it further.

(ii) $M_A < M_h/2$ and small $\tan\beta$: In this case, one can solve the requirement $C_{hAA} = 0$ for λ_1. The exact solution can be read off from Eq. (A3). We provide the solution here for $c_{\beta\alpha} = 0$,

$$\lambda_1 = \frac{M_h^2}{v^2}\left(1 - \frac{t_\beta^2}{2}\right) + \left(\frac{M_H^2 - M_A^2}{v^2}\right)t_\beta^2 - \frac{3}{2}\lambda_6 t_\beta + \frac{1}{2}\lambda_7 t_\beta^3. \tag{12}$$

We checked that even if we allow $C_{hAA} \neq 0$, no significant deviations from relations (11) or (12) are experimentally allowed if $M_A < M_h/2$. Hence we will always impose these relations exactly and fix either $c_{\beta\alpha}$ or λ_1 in terms of these relations if $M_A < M_h/2$.

B. Constraints on the lepton Yukawa coupling ζ_l

Next we present the upper limits on $|\zeta_l|$, the lepton Yukawa coupling parameter in the flavor-aligned 2HDM. This parameter governs in particular the couplings Y_l^A of A to τ-leptons or muons. After earlier similar studies in Ref. [25], precise limits on ζ_l have been obtained in Ref. [23] for the case of the type X model, where $\zeta_l = -\tan\beta$. We have repeated the analysis for the case of the flavor-aligned model, finding essentially the same upper limit on $|\zeta_l|$ as Ref. [23] finds on $\tan\beta$ (except at small M_A due to additional collider constraints; see below).[3]

The upper limits on $|\zeta_l|$ arise on the one hand from experimental constraints on the τ-decay mode $\tau \to \mu\nu_\tau\bar{\nu}_\mu$ versus other decay modes and on leptonic Z-boson decays. 2HDM diagrams contributing to these decays involve tree-level or loop exchange of A or $H^\pm$. They are enhanced by ζ_l and lead to disagreement with observations if $|\zeta_l|$ is too large. We computed the τ- and Z-boson decays and the $\Delta\chi^2$ corresponding to the deviation from experiment as described in Ref. [23] and Sec. II B.

On the other hand, further constraints on ζ_l arise from collider data. In particular, for small M_A ($5 < M_A < 20$ GeV) the upper bound of $|\zeta_l|$ is dominated by the LEP process $ee \to \tau\tau(A) \to \tau\tau(\tau\tau)$ which was probed by the DELPHI Collaboration [46]. In this decay, the electron positron pair annihilates into a Z-boson which further generates a pair of τ-leptons. From one of those, a short-lived A boson is created in resonance, producing finally two more taus.

Our resulting upper limits on $|\zeta_l|$ are shown in Fig. 1 as functions of M_A for various choices of $M_{H^\pm}$. The limits are generally between $|\zeta_l| < 40$ and $|\zeta_l| < 100$. In most of the parameter space the limits are dominated by the τ-decay constraints, which become weaker for larger M_A and larger M_H, $M_{H^\pm}$. The constraints from Z-boson decays become dominant for heavy Higgs masses above around 250 GeV. For even higher Higgs masses, these limits reduce the maximum $|\zeta_l|$ (see the black lines in Fig. 1). Aiming for the largest possible Yukawa couplings, the Z-boson decay constraints imply that even larger heavy Higgs masses will not help. The constraints from LEP data are dominant for small $M_A < 20$ GeV and significantly reduce the maximum $|\zeta_l|$ in this parameter region.

C. Constraints on the up-type Yukawa coupling ζ_u

In this subsection we present the upper limits on ζ_u, the parameter for up-type quark Yukawa couplings. This is a

[2]In the case of the wrong-sign Yukawa limit (see below), the lhs is exactly 2. Still, the approximate form of Eq. (10) holds in this case.

[3]Small differences also arise due to our slightly different treatment of the statistical significances.

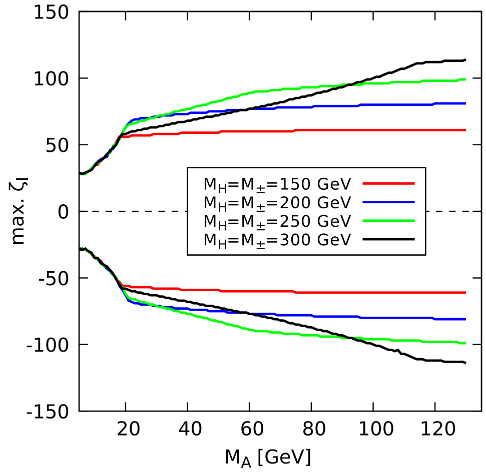

FIG. 1. Maximum possible values of the lepton Yukawa parameter ζ_l, given constraints from τ- and Z-decays and collider data, as a function of M_A for several values of $M_H = M_{H^\pm}$ as indicated.

central part of our analysis, showing characteristic differences between the case of the type X model and the general flavor-aligned model. In what follows, we will focus on negative ζ_l (like in the type X model where $\zeta_l = -\tan\beta$) and positive ζ_u, which leads to larger contributions to a_μ.

In type II or type X models ζ_u is always small for large lepton Yukawa coupling, because $\zeta_u = -1/\zeta_l = 1/\tan\beta$. However, if general Yukawa couplings are allowed, ζ_u can be larger. The maximum possible value is interesting not only for $g-2$ but also in view of future LHC searches for a low-mass A.

We find that ζ_u, in the scenario of $M_A < M_h$ and large ζ_l, is constrained in a complementary way by B-physics on the one hand and by LHC data on the other hand.

Beginning with B-physics, the most constraining observables for this scenario are $b \to s\gamma$ and $B_s \to \mu^+\mu^-$. The sample diagrams shown in Fig. 2 illustrate that the 2HDM predictions depend on combinations of all Yukawa parameters ζ_l, ζ_u, ζ_d and on the Higgs masses M_A and $M_{H^\pm}$. We have implemented the analytical results for the predictions presented in Refs. [47,48] (the authors of Ref. [48] also considered further observables, which however do not constrain the parameter space further; see also Ref. [49] for improvements on the precision of B-physics observables).

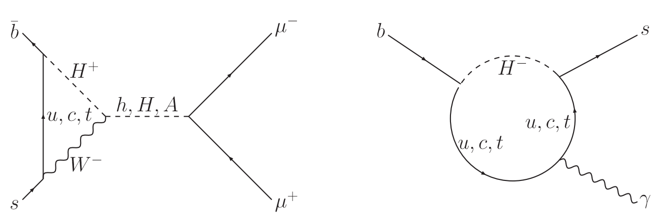

FIG. 2. Sample Feynman diagrams for the processes $B_s \to \mu^+\mu^-$ and $b \to s\gamma$, which depend on the Yukawa couplings of up- and down-type quarks and leptons.

To illustrate the interplay between the observables we show first Fig. 3. It shows the 2σ regions in the ζ_u–ζ_d-plane allowed by either $b \to s\gamma$ or $B_s \to \mu^+\mu^-$ alone or by the combination. In the figure, the representative values $M_{H^\pm} = 200$ GeV, and $(M_A, \zeta_l) = (40\text{ GeV}, -60)$ or $(50\text{ GeV}, -40)$ are fixed, as indicated.

Both observables on their own would allow values of $\zeta_u \gg 1$, by fine-tuning ζ_d and ζ_u. However, the combination of both observables implies an upper limit on ζ_u, which in this case is $\zeta_u < 0.5$.[4]

By performing a similar analysis repeatedly, we obtain maximum values of ζ_u as a function of M_A, $M_{H^\pm}$ and ζ_l. The result will be shown below in the plots of Fig. 4 as continuous lines. Each solid line corresponds to the maximum allowed value (by B-physics) of ζ_u, as a function of M_A and for fixed values of $M_{H^\pm}$ and ζ_l. The dependence on M_A, $M_{H^\pm}$ and ζ_l is mild. Generally, the upper limit on ζ_u is between 0.3 and 0.6.

Turning to LHC Higgs physics, the dashed lines in the plots of Fig. 4 show the maximum ζ_u allowed by LHC collider constraints. These constraints on ζ_u arise from several processes and measurements:

(i) $pp \to A \to \tau\tau$ for $M_A > M_Z$ [50]. In our scenario A decays essentially to 100% into $\tau\tau$. Hence the measurement constrains the production rate of A, which proceeds via top-quark loop and gluon fusion and is thus governed by ζ_u. Hence this measurement provides an essentially universal upper limit of approximately $\zeta_u < 0.2$ which becomes valid above $M_A > 100$ GeV.

(ii) $pp \to H \to \tau\tau$ [50] if $H \to AA$ is kinematically forbidden. Similar to the previous case, H is produced in gluon fusion via a top loop, so its production rate is governed by ζ_u; it decays essentially always into a τ-pair. Hence, again, this measurement places an essentially universal upper limit on ζ_u, valid if $M_A > M_H/2$. In the plots, this limit can be seen for $M_H = 150$ GeV and $M_A > 75$ GeV.

(iii) $pp \to H \to \tau\tau$ [50] if $H \to AA$ is kinematically allowed. This case is relevant in the largest region of parameter space, including the regions with the peak structures in which the collider limits become rather weak and ζ_l-dependent. The scalar Higgs H is produced in gluon fusion via a top loop, so its production rate is governed by ζ_u; its two most important decay modes are $H \to AA$ and $H \to \tau\tau$. Hence, the signal strength for the full process depends not only on ζ_u but also on the triple Higgs coupling C_{HAA}, which is strongly correlated with $C_{HH^+H^-}$ given in Eq. (A1). The signal strength can be

[4]For some values of M_A, $M_{H^\pm}$, separate "islands" in the ζ_u–ζ_d-plane at higher ζ_u can be allowed. They can be excluded by the universal bound $|\zeta_u| < 1.2$ derived from R_b in Ref. [32] and by the similar bound derived from ΔM_s in Ref. [48].

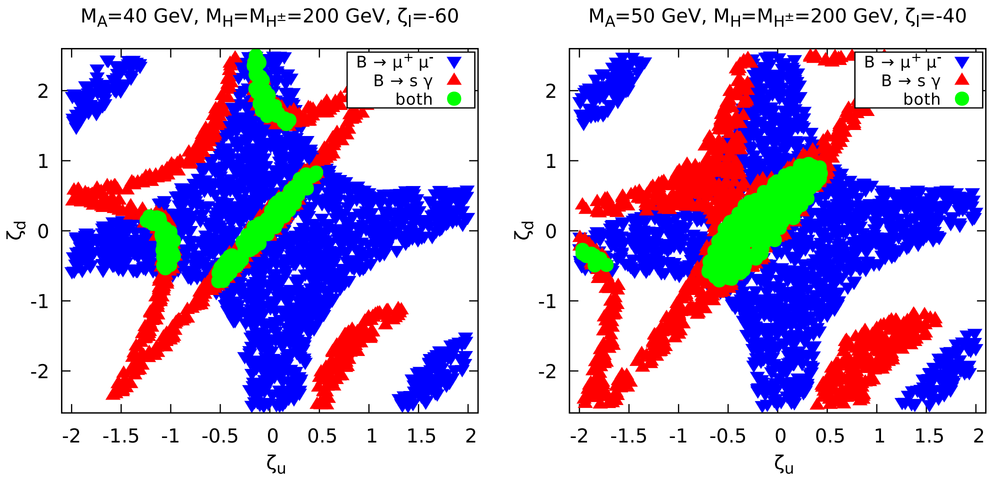

FIG. 3. Allowed parameter regions in the ζ_u–ζ_d-plane given constraints from $b \to s\gamma$ or $B_s \to \mu^+\mu^-$ or the combination. The parameters are chosen as indicated.

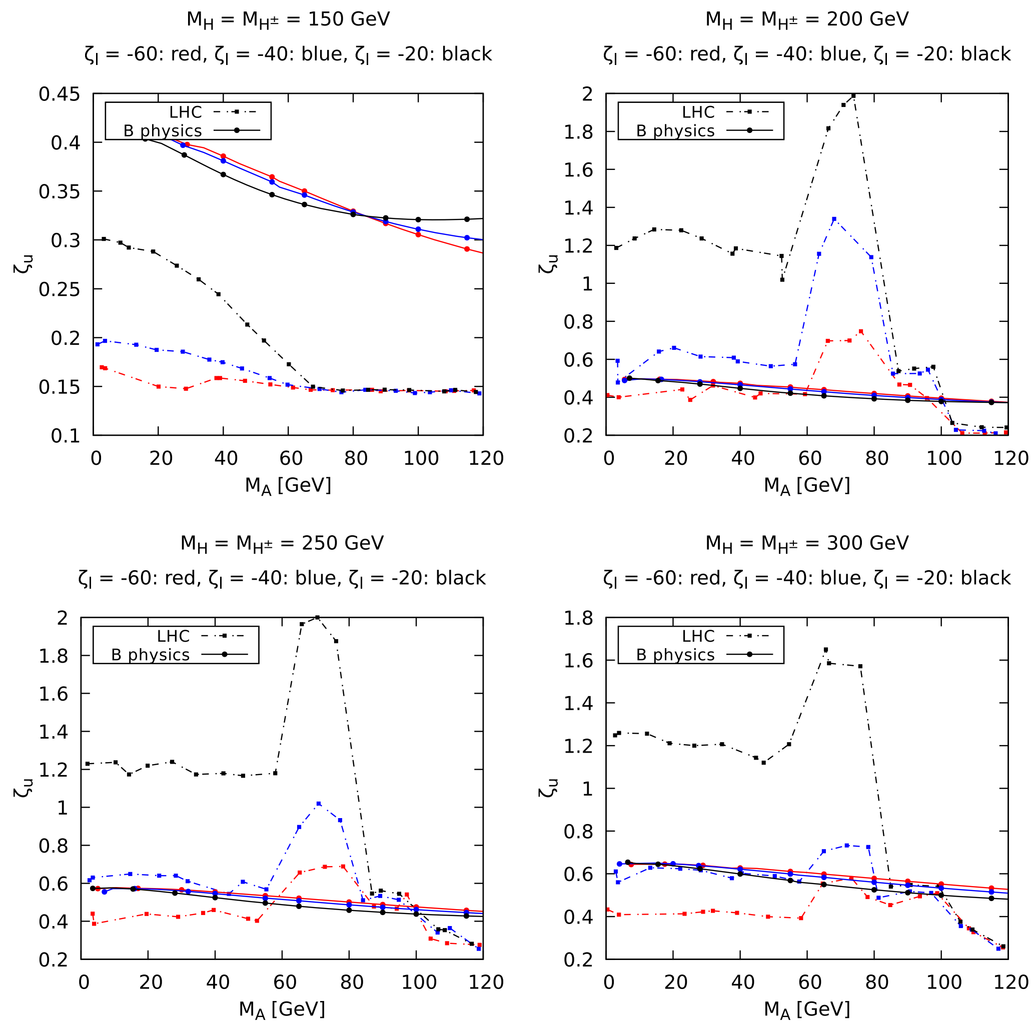

FIG. 4. The maximum allowed values of ζ_u as a function of M_A, for different values of M_H, $M_{H^\pm}$ and ζ_l as indicated. The continuous lines correspond to the upper limit derived from B-physics alone, and the dashed lines to the upper limit derived from LHC Higgs physics alone.

suppressed by small ζ_u (which suppresses the production) or by large $C_{HH^+H^-}$ (which suppresses the decay to $\tau\tau$).

Hence we show the allowed ranges of ζ_u and the triple Higgs coupling $C_{HH^+H^-}$ in Fig. 5, for the representative values $M_A = 50/80$ GeV, $M_H = M_{H^\pm} = 200$ GeV, $\zeta_l = -40$. The colors indicate the successive application of constraints from the electroweak S, T, and U parameters; HiggsBounds; HiggsSignals; and tree-level stability, unitarity and perturbativity (as implemented in 2HDMC [40]). The border of the yellow region shows clearly the correlation between the two couplings mentioned above that is needed to evade the constraints from $pp \to H \to \tau\tau$ searches. The larger the triple Higgs coupling, the larger ζ_u can be. However, perturbativity restricts the triple Higgs coupling, and this restriction depends on whether $M_A < M_h/2$ holds or not. If $M_A < M_h/2$, the relation (12) obtained by setting Eq. (A3) to zero has to be used, and the maximum triple Higgs coupling and thus the maximum ζ_u is smaller.

As a result of this combination of constraints, the LHC Higgs limits on ζ_u are rather loose for M_A between $M_h/2$ and around M_Z (explaining the peaks in Fig. 4), and stronger for lower M_A. The precise value of the limits depends on ζ_l, which also influences the branching ratio $H \to \tau\tau$.

(iv) We also mention the analysis of Ref. [27], where LHC constraints on the type X model have been studied; since ζ_u is negligible in the type X model, those constraints are weaker than the ones we consider here, and they do not limit ζ_u. Still, that analysis shows that data from multi-Higgs production followed by decays into multi-τ final states lead to interesting (mild) constraints on heavy M_H, $M_{H^\pm}$.

IV. BOSONIC CONTRIBUTIONS TO a_μ AND RELEVANT PARAMETER CONSTRAINTS

As discussed in the previous section, the 2HDM parameter region of interest for a_μ is characterized by large Yukawa coupling parameter ζ_l and small pseudoscalar mass M_A. The bosonic two-loop contributions a_μ^{B} computed in Ref. [30] depend on a large number of additional parameters: the physical Higgs masses M_H, $M_{H^\pm}$; the mixing angle $c_{\beta\alpha}$; $\tan\beta$; and the Higgs potential parameters λ_1 and $\lambda_{6,7}$. In the present section we provide an overview of the influence of these parameters, constraints on their values, and update the analysis of Ref. [30] given those constraints. As a result we derive the maximum possible values of the bosonic two-loop contributions to a_μ.

The bosonic two-loop contributions can be split into three parts [30],

$$a_\mu^{\mathrm{B}} = a_\mu^{\mathrm{EW\ add}} + a_\mu^{\mathrm{non\text{-}Yuk}} + a_\mu^{\mathrm{Yuk}}, \tag{13}$$

where $a_\mu^{\mathrm{EW\ add}}$ denotes the difference between the contribution of the SM-like Higgs in the 2HDM and its SM counterpart; $a_\mu^{\mathrm{non\text{-}Yuk}}$ and a_μ^{Yuk} denote remaining bosonic contributions without/with Yukawa couplings.

We begin with a discussion of $a_\mu^{\mathrm{EW\ add}}$, which is approximately given by $a_\mu^{\mathrm{EW\ add}} = 2.3\times 10^{-11} c_{\beta\alpha}\zeta_l$. As discussed in Sec. III A, the product $c_{\beta\alpha}\zeta_l$ is restricted by Higgs signal strength measurements to be smaller than unity. Hence this product can never be an enhancement factor. Specifically, as a result we obtain the conservative limit

$$|a_\mu^{\mathrm{EW\ add}}| < 0.2\times 10^{-10}, \tag{14}$$

such that these contributions are negligible.

Next we consider $a_\mu^{\mathrm{non\text{-}Yuk}}$, the contribution from diagrams in which the extra 2HDM Higgs bosons couple only

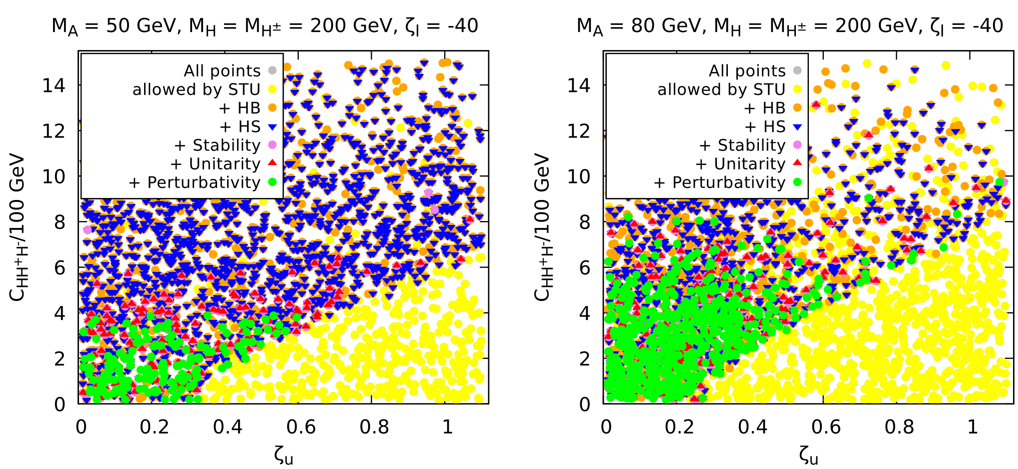

FIG. 5. Allowed ranges of ζ_u and the triple Higgs coupling $C_{HH^+H^-}$, given certain constraints; see legend and text. The constraints are applied successively. The scanned parameter space is defined by Eq. (7), with Eq. (12) in the case $M_A < M_h/2$.

to SM gauge bosons and not to fermions. Similar to the quantity $\Delta\rho$, this contribution is enhanced by large mass splittings $|M_H - M_{H^\pm}|$ between the heavy Higgs bosons. Conversely, constraints on $\Delta\rho$ restrict this mass splitting [22,51] and thus $a_\mu^{\text{non-Yuk}}$. We find that $a_\mu^{\text{non-Yuk}}$ is similarly negligible as Eq. (14).

Finally we turn to a_μ^{Yuk}, the potentially largest bosonic two-loop contribution. The authors of Ref. [30] decomposed this contribution into several further subcontributions depending on the appearance of triple Higgs couplings, the mixing angle $c_{\beta\alpha}$ and the Yukawa parameter ζ_l. Among these parameters, the product $c_{\beta\alpha}\zeta_l$ is restricted as discussed above; furthermore, the triple Higgs couplings are constrained by perturbativity. Inspection of the results of Figs. 5 and 6 of Ref. [30] then shows that all subcontributions to a_μ^{Yuk} are at most of the order 10^{-11}, with the exception of the ones enhanced by the triple Higgs coupling $C_{HH^+H^-}$.

Hence the overall bosonic two-loop contributions are essentially proportional to the value of the coupling $C_{HH^+H^-}$. Likewise, all the parameters $\tan\beta$, $\lambda_{1,6,7}$ enter the prediction for a_μ essentially via this coupling. This proportionality is shown in Fig. 6(a), which displays the ratio ρ, defined via

$$|a_\mu^{\text{B}}| = \rho |C_{HH^+H^-}/\text{GeV}||\zeta_l| \times 10^{-15} \qquad (15)$$

as a function of a_μ^{B} in a scan of parameter space. The approximate proportionality clearly emerges, if a_μ^{B} is larger than around 0.5×10^{-10}. The quantity ρ then only depends on the heavy Higgs masses, and its value is $\rho \approx 6, 3, 2, 1$ (for $M_H = M_{H^\pm} = 150$, 200, 250, 300 GeV, respectively). In Fig. 6(a) we display only positive a_μ^{B}. The sign of a_μ^{B} also depends on the triple Higgs coupling (see the explicit formula in the Appendix). For small $c_{\beta\alpha}$ it is thus determined essentially by $(\tan\beta - 1)$. If $\tan\beta < 1$, a_μ^{B} is positive (for negative ζ_l and with small corrections if $c_{\beta\alpha} \neq 0$).

Hence we mainly need to discuss the behavior of the coupling $C_{HH^+H^-}$. We need to distinguish two cases:

(i) 2HDM type I, II, X, and Y: Here $\tan\beta$ and the Yukawa parameters are correlated. Specifically in the most interesting case of the type X model, $\tan\beta = -\zeta_l$ and is therefore large. As a result, the triple Higgs coupling is suppressed, and the overall bosonic contribution a_μ^{B} is negligible.

(ii) General aligned 2HDM: In this case $\tan\beta$ is independent of ζ_l, and the triple Higgs coupling $C_{HH^+H^-}$ can be largest if $\tan\beta = \mathcal{O}(1)$.

Focusing now on the second case of the aligned 2HDM, the range of possible values of $C_{HH^+H^-}$ can already be seen in Fig. 5 for particular choices of $M_A = 50/80$ GeV, $M_H = M_{H^\pm} = 200$ GeV, $\zeta_l = -40$. There, large $C_{HH^+H^-}$ was important to suppress the branching ratio of $H \to \tau\tau$ and allow large values for ζ_u. For $M_A = 80$ GeV all parameters $\lambda_{1,6,7}$ and $\tan\beta$ have been varied in the full range of Eq. (7), and the maximum allowed triple Higgs coupling is around 1000 GeV. For $M_A = 50$ GeV, on the other hand, λ_1 is fixed as explained in Sec. III A to suppress the decay $h \to AA$. Hence the maximum triple Higgs coupling is smaller, in this case around 400 GeV.

The results generalize to other values of M_A. The maximum triple Higgs coupling essentially only depends on whether M_A is smaller or larger than $M_h/2$. In the latter case, the triple Higgs coupling reaches around 1000 GeV, and in the former case only around 400–600 GeV, depending on the heavy Higgs masses M_H, $M_{H^\pm}$.

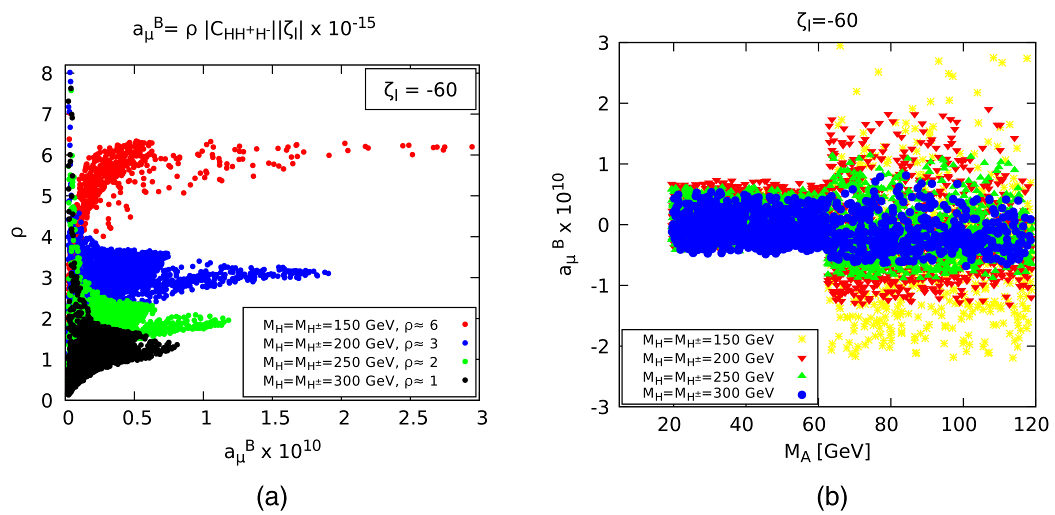

FIG. 6. The bosonic contributions a_μ^{B}. (a) The proportionality factor ρ defined in Eq. (15) for a scan of parameter space with different values of the heavy Higgs masses. (b) The range of possible values for a_μ^{B}. The scanned parameter space is defined by Eq. (7), with Eq. (12) in the case $M_A < M_h/2$. Only points passing all constraints of Sec. III are shown. Plot (a) would remain essentially the same for other choices of ζ_l, and plot (b) would change essentially linearly with ζ_l. In plot (b), part of the region below $M_A < 20$ GeV is excluded for $\zeta_l = -60$, corresponding to the limit in Fig. 1.

Figure 6(b) shows the range of possible bosonic contributions $a_\mu^{\rm B}$ as a function of M_A for various values of $M_H = M_{H^\pm}$. The result is fully understood with the proportionality (15) and the maximum values for $C_{HH^+H^-}$ just discussed. We display the result only for a particular value of ζ_l but we have checked that the results are exactly linear in ζ_l as expected. We have also checked that the maximum results do not change significantly if the heavy Higgs masses are varied independently, $M_H \neq M_{H^\pm}$, or if $\lambda_{6,7}$ are set to zero.

As a result of the analysis of the individual contributions to $a_\mu^{\rm B}$ and of $C_{HH^+H^-}$ we can now summarize the maximum possible $a_\mu^{\rm B}$ in the simple approximation formula

$$|a_\mu^{\rm B}|^{\rm max} \approx \begin{Bmatrix} 1 \\ 0.5 \end{Bmatrix} \rho |\zeta_l| \times 10^{-12} \tag{16}$$

where the upper (lower) result holds for $M_A > M_h/2$ ($< M_h/2$) and where $\rho = 6,\ 3,\ 2,\ 1$ for $M_H = M_{H^\pm} = 150,\ 200,\ 250,\ 300$ GeV, respectively.

V. MUON $g-2$ IN THE 2HDM

In this section we use the previous results on limits on relevant parameters to discuss in detail the possible values of a_μ in the 2HDM, answering the two questions raised in the Introduction. Section V A discusses a_μ as a function of the relevant parameters and characterizes parameter regions giving particular values for a_μ; Sec. V B provides the maximum a_μ that can be obtained in the 2HDM overall or for certain parameter values.

Before entering details, we provide here useful approximation formulas for a_μ in the 2HDM, which provide the correct qualitative behavior in the parameter region of interest with small M_A and large lepton Yukawa coupling ζ_l. The one-loop contributions $a_\mu^{\rm 2HDM,1}$ are dominated by diagrams with A exchange; the fermionic two-loop contributions $a_\mu^{\rm F}$ are dominated by diagrams with τ-loop and A exchange or top-loop and A, H, $H^\pm$ exchange; the bosonic two-loop contributions $a_\mu^{\rm B}$ are dominated by diagrams with H exchange and $H^\pm$-loop. The numerical approximations for these contributions are, using $\hat{x}_S \equiv M_S/100$ GeV and $M_{H^\pm} = M_H$,

$$a_\mu^{\rm 2HDM,1} \simeq \left(\frac{\zeta_l}{100}\right)^2 \left\{\frac{-3-0.5\ln(\hat{x}_A)}{\hat{x}_A^2}\right\} \times 10^{-10}, \tag{17a}$$

$$a_\mu^{\rm F\tau} \simeq \left(\frac{\zeta_l}{100}\right)^2 \left\{\frac{8+4\hat{x}_A^2+2\ln(\hat{x}_A)}{\hat{x}_A^2}\right\} \times 10^{-10}, \tag{17b}$$

$$a_\mu^{\rm Ft} \simeq \left(\frac{-\zeta_l\zeta_u}{100}\right) \{22-14\ln(\hat{x}_A)+32-15\ln(\hat{x}_H)\} \times 10^{-10}, \tag{17c}$$

$$|a_\mu^{\rm B}| \simeq \rho |C_{HH^+H^-}/{\rm GeV}| |\zeta_l| \times 10^{-15}. \tag{17d}$$

The sign of the τ-loop contribution is positive in our parameter region; the one-loop contributions are negative but are subdominant except at very small M_A. The top-loop contribution is positive if ζ_u has a sign opposite to ζ_l, which is why we choose $\zeta_l < 0$ and focus on $\zeta_u > 0$. $a_\mu^{\rm B}$ is positive if $\zeta_l < 0$ and $\tan\beta < 1$ (up to small corrections if $a_\mu^{\rm B}$ is small); see Sec. IV for further details on the quantity ρ and the approximation for $a_\mu^{\rm B}$.

For the exact results we refer to the literature. The full two-loop result has been obtained and documented in Ref. [30], the full set of Barr-Zee diagrams has been obtained in Ref. [29], and for earlier results we refer to the references therein. In our numerical evaluation we use the results of Ref. [30].

A. a_μ in different parameter regions

Here we discuss the question raised in the Introduction: In which parameter region can the 2HDM accommodate the current deviation in a_μ (or a future, possibly larger or smaller deviation)?

We begin by listing several remarks which can be obtained from the results of the previous sections.

(i) All important contributions to a_μ are proportional to the lepton Yukawa coupling parameter ζ_l or ζ_l^2 (where e.g., in the type X model $\zeta_l = -\tan\beta$). Hence ζ_l must be much larger than unity in order to obtain significant a_μ. From Sec. III C we then obtain that the quark Yukawa parameters ζ_u, ζ_d can be at most of order unity.

This implies that the bottom loop contribution is negligible, and that the type X model is the only one of the usual four discrete symmetry models with significant a_μ (see also Ref. [22]).

(ii) The single most important contribution to a_μ is the one from the τ-loop; see Eq. (17). It depends on ζ_l and M_A. In the general flavor-aligned model, the top-loop contribution can also be significant provided ζ_u is close to its maximum value of order unity.

(iii) The masses of the heavy Higgs bosons H and $H^\pm$ are relatively unimportant for a_μ. However, they are important for the limits on the possible values of ζ_l and ζ_u. If these Higgs bosons have masses around 250 GeV the largest $|\zeta_l|$ up to 100 are allowed in most of the parameter space. For even higher masses the limits on $|\zeta_l|$ become slightly stronger and the limits on ζ_u saturate thanks to Z-decay and LHC search limits.

(iv) The mass splitting between M_H and $M_{H^\pm}$ is unimportant. It is strongly restricted by limits from electroweak precision observables [22,51] and we have checked that its remaining influence on the limits on ζ_l, ζ_u and on the bosonic contributions $a_\mu^{\rm B}$ is negligible. Hence we set $M_H = M_{H^\pm}$ in all our numerical examples.

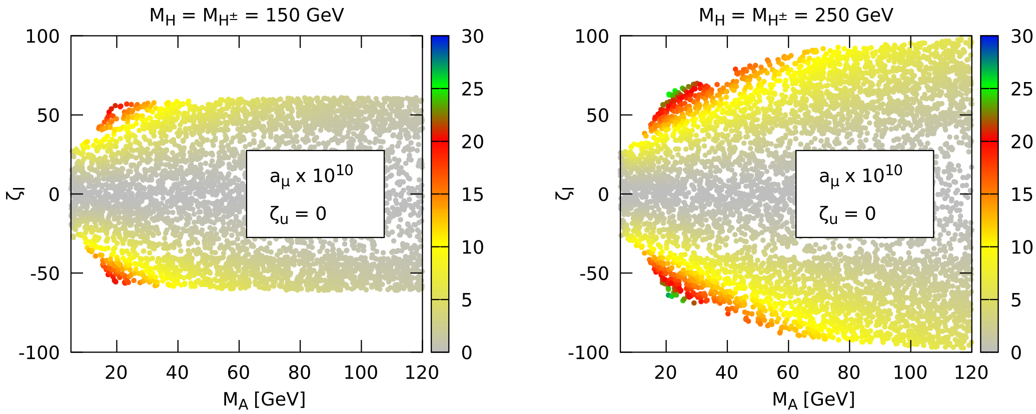

FIG. 7. a_μ in the 2HDM (from two-loop fermionic and one-loop contributions, and in units of 10^{-10}), as a function of M_A and the τ-Yukawa parameter ζ_l; the current deviation (1) corresponds to green points. Only points in the allowed region of Fig. 1 are shown. The parameter ζ_u is set to zero, corresponding to the case with vanishing top-loop contributions and approximately to the type X model case. The parameters M_H, $M_{H^\pm}$ are fixed as indicated. Corresponding plots with M_H, $M_{H^\pm} = 200$, 300 GeV would look very similar, except for the slightly different allowed regions.

(v) The Higgs mixing angle $c_{\beta\alpha}$ is unimportant for a_μ. For our scenario of interest it is mostly limited by LHC measurements of Higgs couplings to leptons, which restrict $|c_{\beta\alpha}\zeta_l|$ to be smaller than order one. Hence all contributions to a_μ depending on $c_{\beta\alpha}$ are strongly suppressed.

(vi) The parameters $\lambda_{1,6,7}$ and $\tan\beta$ from the Higgs potential appear in a_μ essentially only via the triple Higgs coupling $C_{HH^+H^-}$, which in turn is maximized for $\tan\beta = \mathcal{O}(1)$. In the type X model with large $\tan\beta = -\zeta_l$ this strongly suppresses the bosonic contributions a_μ^{B}; in the more general aligned model, the bosonic diagrams behave as given in Eq. (17d).

In the plots of this subsection we do not include the bosonic contributions a_μ^{B} because their parameter dependence is clear from this discussion, because their sign can be positive or negative, and because their numerical impact is small.

Figures 7 and 8 show a_μ as a function of the most important parameters M_A, ζ_l and ζ_u and the heavy Higgs masses M_H, $M_{H^\pm}$.

Figure 7 focuses on the two most important parameters M_A and the lepton Yukawa coupling ζ_l. It shows a_μ (including one-loop and fermionic two-loop contributions) as a function of M_A and ζ_l. The top-Yukawa parameter ζ_u is fixed to $\zeta_u = 0$; hence only the τ-loop and the one-loop contributions are significant. The result also corresponds to the type X model, in which ζ_u is negligible. We further fix $M_H = M_{H^\pm} =$ 150, 250 GeV and show only parameter points allowed by the constraints of Sec. III B. The results for a_μ are not very sensitive to the choice of M_H, $M_{H^\pm}$, but for $M_H = M_{H^\pm} =$ 250 GeV the allowed parameter space is largest.

Even at the border of the allowed region, a contribution as large as the deviation (1) can barely be obtained (see also the discussions in Refs. [23,25]). Only in the small corner with $M_A \sim 20$ GeV and $|\zeta_l| \sim 70$, a_μ comes close to explaining

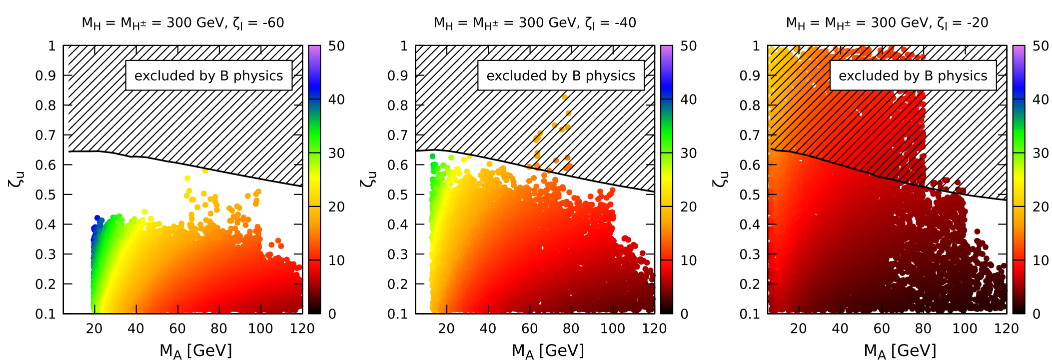

FIG. 8. a_μ in the 2HDM (from two-loop fermionic and one-loop contributions, and in units of 10^{-10}), as a function of M_A and the top-Yukawa parameter ζ_u; the current deviation (1) corresponds to yellow/green points. Only points allowed by the collider constraints of Fig. 4 are shown; the B-physics constraints are shown as the hatched regions. The parameters ζ_l and M_H, $M_{H^\pm}$ are fixed as indicated. Corresponding plots with other choices of M_H, $M_{H^\pm}$ would look very similar, except for the different allowed parameter regions.

Eq. (1). More generally, the plot reflects the behavior that a_μ is dominated by the τ-loop which in turn is approximately proportional to $(\zeta_l/M_A)^2$. A contribution above approximately 20 (in units of 10^{-10}) is possible in the small region where $|\zeta_l/M_A| > 2\ \mathrm{GeV}^{-1}$, which is allowed for around $M_A \sim 20$–40 GeV. Even smaller contributions above 10 are difficult to obtain. They require $|\zeta_l/M_A| > 1\ \mathrm{GeV}^{-1}$ and are possible for M_A up to around 60–80 GeV.

The impact of the top loop for $\zeta_u \neq 0$ can be seen in Fig. 8. It shows a_μ (including one-loop and fermionic two-loop contributions) as a function of M_A and ζ_u. In the plot, ζ_l is fixed to exemplary values $\zeta_l = -20, -40, -60$. Because of the sum of τ and top loops the dependence on ζ_l is nonlinear, and the relative importance of the top loop and thus of the parameter ζ_u is higher for smaller ζ_l.

We display a_μ for all points which pass the collider constraints discussed in Sec. III C, and we display the constraints from B-physics on the maximum ζ_u as a line in the plots. In Fig. 8 we do not show all choices of the heavy Higgs masses M_H, $M_{H^\pm}$ but fix $M_H = M_{H^\pm} = 300$ GeV. Like in the previous figure, the values of a_μ would be essentially independent of the heavy Higgs masses; the behavior of the collider and B-physics constraints can be obtained from Fig. 4.

Nonzero ζ_u helps in explaining the current a_μ deviation (1) of around 30 (in units of 10^{-10}). The fan-shaped structure of the plots shows that higher values of the Higgs mass M_A can be compensated by larger ζ_u to obtain the same a_μ. For instance, for $\zeta_l = -60$, contributions to a_μ around 30 can be obtained up to $M_A \sim 40$ GeV. Contributions above 20 can be obtained up to $M_A \sim M_Z$, by taking advantage of the larger allowed values of ζ_u in this mass range.

For smaller $\zeta_l = -40$, contributions above 20 are possible for M_A up to around 60 GeV, and contributions above 10 are possible up to $A \sim M_Z$. For $\zeta_l = -20$, the contributions to a_μ are generally smaller than 20×10^{-10}, but even here nonzero ζ_u strongly increases a_μ.

B. Maximum possible a_μ in the 2HDM

Now we discuss the question: What is the overall maximum possible value of a_μ that can be obtained in the 2HDM? Figures 9 and 10 show the maximum possible

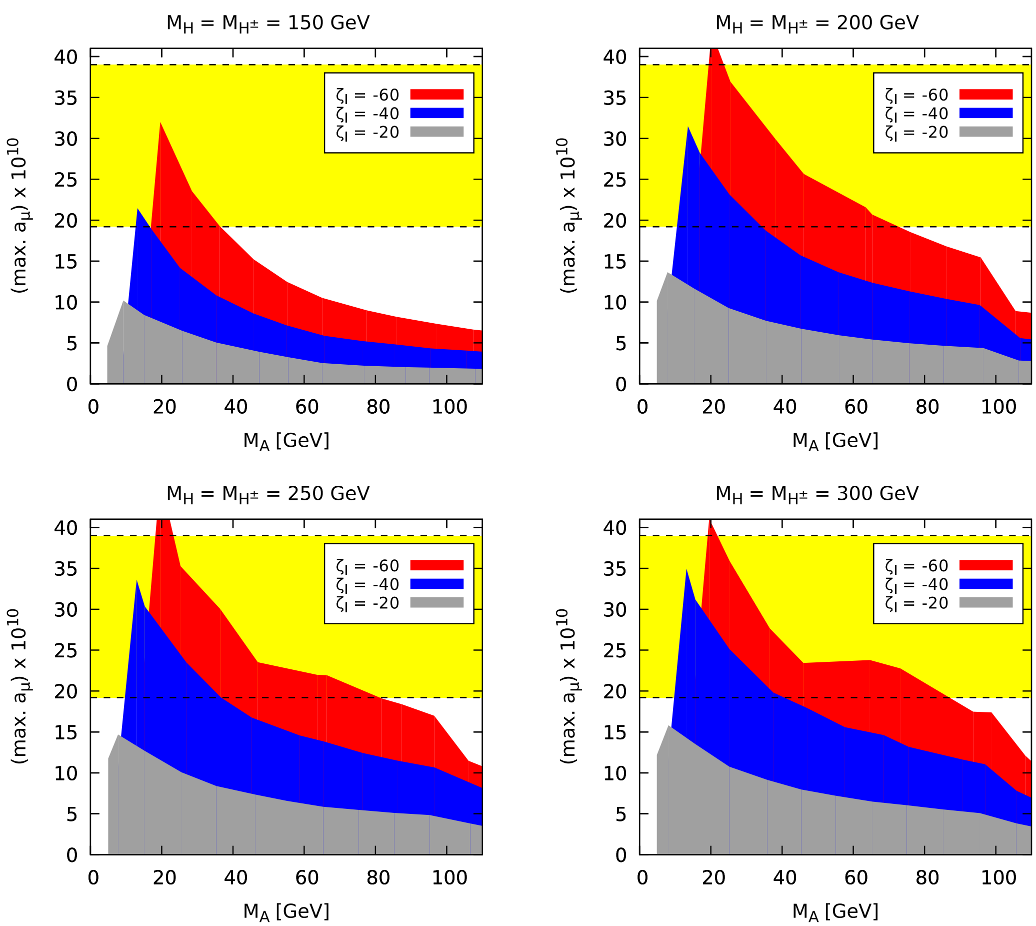

FIG. 9. The maximum a_μ (including one-loop and all two-loop contributions) for several fixed values of ζ_l and $M_H = M_{H^\pm}$. For each M_A and ζ_l, the maximum ζ_u is obtained from the results of Sec. III C. The yellow band indicates the current a_μ deviation, defined by taking the envelope of the 1σ bands given by Eq. (1).

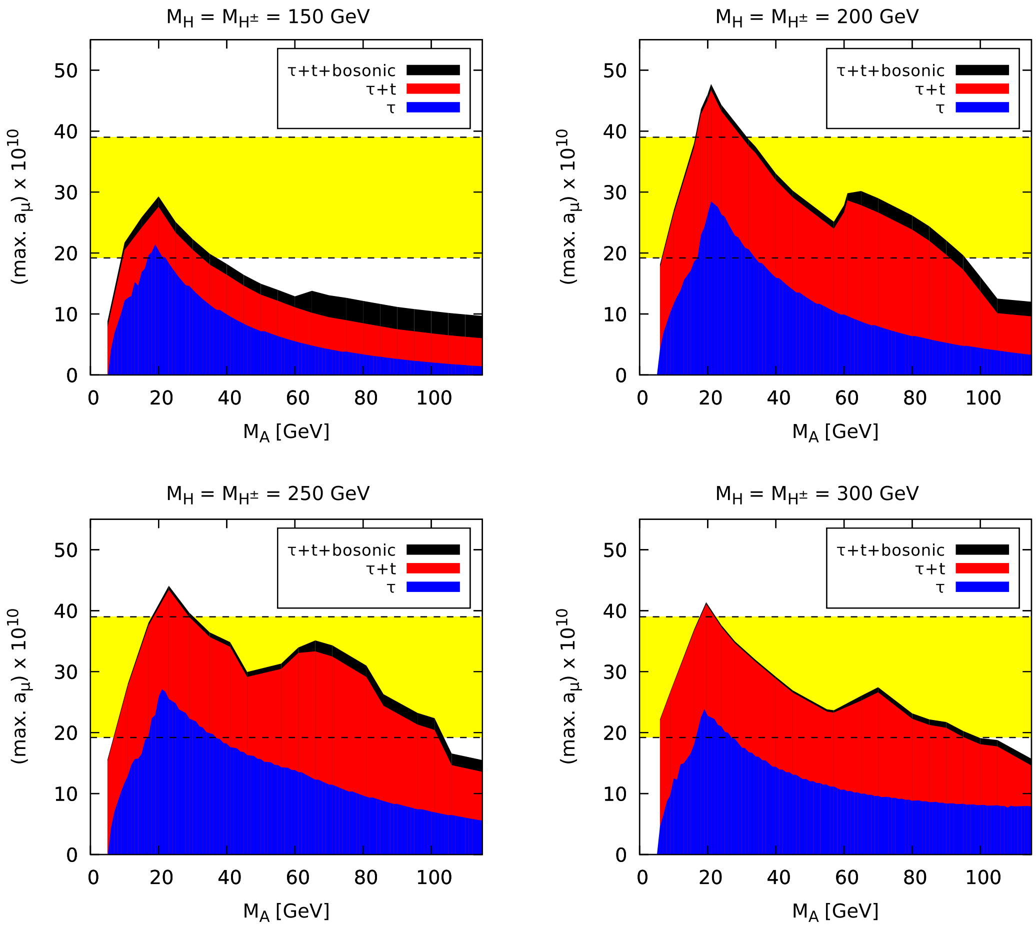

FIG. 10. The overall maximum a_μ (including one-loop and all two-loop contributions) as a function of M_A, for several fixed values of $M_H = M_{H^\pm}$. For each value of M_A, the maximum value of $|\zeta_l|$ is determined as in Sec. III B; then the maximum ζ_u is obtained from the results of Sec. III C. The result without top-loop and bosonic contributions (which would correspond to the maximum in the type X model) is shown in blue; the result without bosonic two-loop contributions in red; the total maximum result, including the maximum bosonic contributions, in black. The yellow band indicates the current a_μ deviation, defined by taking the envelope of the 1σ bands given by Eq. (1).

a_μ in the 2HDM, first for fixed choices of the lepton Yukawa coupling $\zeta_l = -20$, -40, -60, and then overall.

Figure 9 is obtained by maximizing ζ_u for each parameter point, given all constraints discussed in Sec. III C. The plots clearly show the prominent role of M_A and the lepton Yukawa coupling ζ_l. The values of the heavy Higgs bosons M_H, $M_{H^\pm}$ mainly matter because they influence the maximum allowed value of ζ_u. Only two cases need to be clearly distinguished: small M_H, $M_{H^\pm} = 150$ GeV and larger M_H, $M_{H^\pm} = 200$, 250, 300 GeV, which all lead to similar results for a_μ.

For each value of ζ_l, there is a sharp maximum around $M_A \sim 20$ GeV. At the maximum, a_μ obviously depends on ζ_l, but also on the heavy Higgs masses M_H, $M_{H^\pm}$, because their values influence the maximum allowed value of ζ_u. For $\zeta_l = -60(-40)$ and large M_H, $M_{H^\pm}$, a_μ reaches $40(30) \times 10^{-10}$, which is larger than the currently observed deviation (1). For $M_H = M_{H^\pm} = 150$ GeV or $\zeta_l = -20$, the contributions to a_μ are smaller.

For values of M_A lower than at the peaks in Fig. 9, the maximum a_μ values drop sharply (the drop is at lower M_A if ζ_l is smaller). The reason is that for each ζ_l there is a minimum allowed value of M_A mainly because of the collider limits discussed in Sec. III B. Even if lower values of M_A were allowed, a_μ would be suppressed by the negative one-loop contribution.

For higher values of M_A, a_μ is suppressed by M_A. As can be estimated from the approximation (17), the suppression is weaker than $1/M_A^2$. Further the suppression is modulated by the maximum possible value of ζ_u. In particular, above $M_A > M_h/2$, higher values of ζ_u are allowed, and the maximum a_μ drops more slowly with M_A.

In summary, the deviation (1) can be explained at the 1σ level for $M_A = 20$–40 GeV and for $\zeta_l = -40$ and high M_H, $M_{H^\pm}$ or $\zeta_l = -60$ independently of M_H, $M_{H^\pm}$. It can further be explained for $M_A = 20$–80 GeV for $\zeta_l = -60$ if M_H, $M_{H^\pm}$ are high.

The overall maximum a_μ in the flavor-aligned 2HDM can be seen in Fig. 10 for several choices of M_H, $M_{H^\pm}$. The figure is obtained by maximizing first ζ_l (i.e., the τ-loop contribution), then ζ_u (i.e., the top-loop contribution), and finally the bosonic two-loop contribution for each parameter point. All constraints discussed in Secs. III B and III C are employed.

The plots display not only the final total result for a_μ including all one- and two-loop contributions, but also the results of the τ-loop (plus one-loop) contribution alone, and the results including the top-loop but excluding the bosonic two-loop contributions. In this way the plots allow us to read off the results corresponding to the 2HDM type X and to read off the influence of the bosonic two-loop corrections.

Starting the discussion with the type X model result (blue), the plots confirm that the type X model can barely explain the current deviation (1). The largest values that can be obtained are around 27×10^{-10} at $M_A = 20$ GeV for M_H, $M_{H^\pm} = 200$–250 GeV. For higher or lower values of M_A the maximum type X contributions drop quickly, and values above 20×10^{-10} can only be obtained between $M_A = 20$–40 GeV.

Hence going beyond the type X model and allowing general Yukawa couplings significantly widens the parameter space which can lead to significant contributions to a_μ. Both the top-loop and the bosonic two-loop contributions can significantly increase a_μ. Thanks to the behavior discussed in Sec. IV and expressed in Eqs. (17) both of these contributions are not significantly suppressed by heavier M_A. On the contrary, for heavier M_A, larger ζ_u and larger triple Higgs couplings $C_{HH^+H^-}$ are allowed, and the loop functions are not strongly suppressed by heavy M_A.

Thus, in the general (flavor-)aligned 2HDM one can obtain even $a_\mu > 45 \times 10^{-10}$ if $M_A \sim 20$ GeV and if M_H, $M_{H^\pm}$ are in the range 200–250 GeV. Hence the 2HDM could even accommodate a larger deviation than (1), which might be established from forthcoming a_μ measurements. Thanks to the large possible values of the top Yukawa parameter ζ_u, the current deviation can be explained at the 1σ level in the entire range $M_A = 20$–100 GeV.

VI. SUMMARY AND CONCLUSIONS

The 2HDM is a potential source of significant contributions to the anomalous magnetic moment of the muon a_μ, and it could explain the current deviation (1). Here we have provided a comprehensive analysis of the relevant parameter space and of possible flavor-aligned 2HDM contributions to a_μ. Our analysis was kept general, anticipating that future a_μ measurements might further increase or decrease the deviation (1).

The relevant parameter space is characterized by light pseudoscalar Higgs with mass $M_A < 100$ GeV and large Yukawa couplings to leptons. Among the usual 2HDM models with discrete symmetries this is only possible in the lepton-specific type X model. In the type X model, large lepton Yukawa couplings imply negligible quark Yukawa couplings to the A boson. We considered the more general flavor-aligned model, which contains type X as a special case but in which simultaneously significant Yukawa couplings to quarks are possible.

We first investigated the allowed values of the Yukawa coupling parameters ζ_l and $\zeta_{u,d}$ (which would be given by $-\tan\beta$ and $1/\tan\beta$ in the type X model). An extensive summary of the results is provided at the beginning of Sec. V A. In short, the lepton Yukawa coupling $|\zeta_l|$ can take values up to 40–100, depending on the values of all Higgs masses. For very light $M_A < 20$ GeV, very severe limits from LEP data reduce the maximum $|\zeta_l|$ and thus the maximum a_μ. For large lepton Yukawa coupling, both quark Yukawa couplings $\zeta_{u,d}$ can be $\mathcal{O}(0.5)$ at most because of B-physics data and LHC Higgs searches. While ζ_d has negligible influence on a_μ, in particular the upper limit on the top Yukawa coupling ζ_u is critical for a_μ. Interestingly, for $M_A > M_h/2$ GeV, slightly larger values of ζ_u are allowed thanks to an interplay between the triple Higgs couplings and the Yukawa coupling.

As an intermediate result and an update of the results of Ref. [30] on the full two-loop calculation of a_μ in the 2HDM, we evaluated the maximum contributions a_μ^{B} from bosonic two-loop diagrams. Going beyond the type X model can also increase a_μ^{B}. The maximum is mainly determined by the maximum triple Higgs coupling, which is obtained if $\tan\beta \ll |\zeta_l|$. It reaches 3×10^{-10} if ζ_l is also maximized and if M_A is around 100 GeV and the heavy Higgs masses M_H, $M_{H^\pm}$ are not much higher.

Figures 7, 8, 9, and 10 answer the questions of how a_μ depends on the 2HDM parameters and what the maximum a_μ is that can be obtained in the 2HDM. The overall maximum is above 45×10^{-10}, and it can be obtained for $M_A \sim 20$ GeV. More generally contributions significantly above the current deviation (1) can be obtained for M_A up to 40 GeV. Thanks to the large allowed top Yukawa coupling, the current deviation (1) can be explained at the 1σ level for M_A up to 100 GeV. Even if the lepton Yukawa coupling is not maximized but fixed at only $\zeta_l = -40$, a 1σ explanation is possible up to $M_A = 40$ GeV. The heavy Higgs masses M_H and $M_{H^\pm}$ are not very critical; the maximum a_μ is obtained if they are in the range 200–300 GeV; for lower or higher masses the limits on the Yukawa couplings become stronger, and significantly higher masses are disfavored by triviality constraints [22,25].

For the type X model, the maximum contributions are significantly smaller, only slightly above 25×10^{-10}. A 1σ explanation of the current deviation is only possible in the small range of M_A between 20 and 40 GeV, and even a potential future deviation of only 10×10^{-10} can be explained only for $M_A < 80$ GeV.

It is of high interest to test this parameter space more fully at the LHC. In view of the significant couplings of the low-mass A boson to τ leptons and top quarks, it is promising to derive more stringent upper limits on these couplings, particularly on the product $|\zeta_l \zeta_u|$. Such more stringent limits will have immediate impact on the possible values of a_μ in the 2HDM. At the same time, the future a_μ measurements have a high potential to constrain the 2HDM parameter space. In particular the type X model might be excluded by a confirmation of a large a_μ deviation, and in the more general model, lower limits on the top Yukawa coupling and upper limits on M_A might be derived.[5]

ACKNOWLEDGMENTS

We gratefully acknowledge discussions with Jinsu Kim, Eung Jin Chun, Wolfgang Mader, Mikolaj Misiak, and Rui Santos. The authors acknowledge financial support from DFG Grant No. STO/876/6-1, and CAPES (Coordenação de Aperfeiçoamento de Pessoal de Nível Superior), Brazil. The work has further been supported by the high-performance computing cluster Taurus at ZIH, TU Dresden, and by the National Science Center, Poland, through the HARMONIA project under Contract No. UMO-2015/18/M/ST2/00518 (2016-2019).

APPENDIX: EXPLICIT RESULTS FOR TRIPLE HIGGS COUPLINGS

Here we provide the explicit results for the triple Higgs couplings which are required for our analysis of the maximum allowed values of $C_{HH^+H^-}$ in Sec. III C and the maximum possible values of a_μ^{B} in Sec. IV. We first present full formulas in the generic basis, and then we present useful approximation formulas valid in the Higgs basis.

The triple Higgs couplings of the heavy Higgs H to either AA or $H^\pm H^\mp$ are correlated as

$$C_{HH^+H^-} = C_{HAA} - 2\left(\frac{M_{H^\pm}^2 - M_A^2}{v}\right) c_{\beta\alpha}, \tag{A1}$$

and in the generic basis C_{HAA} is given by

$$\begin{aligned} C_{HAA} = {}& \lambda_1 v \left(s_{\beta\alpha} \frac{1-t_\beta^2}{t_\beta^3} - c_{\beta\alpha} \frac{2}{t_\beta^2} \right) + s_{\beta\alpha} \frac{M_h^2}{v} \frac{t_\beta^2 - 1}{t_\beta^3} + c_{\beta\alpha} \left(\frac{M_h^2}{v} \frac{2+t_\beta^2}{t_\beta^2} - 2\frac{M_A^2}{v} \right) \\ & + c_{\beta\alpha} \frac{M_h^2 - M_H^2}{v} \left(\frac{2}{t_\beta^2} - 3 + c_{\beta\alpha} s_{\beta\alpha} \frac{1-6t_\beta^2 + t_\beta^4}{t_\beta^3} + 4c_{\beta\alpha}^2 \frac{t_\beta^2 - 1}{t_\beta^2} \right) + \lambda_6 v \left(s_{\beta\alpha} \frac{2-t_\beta^2}{t_\beta^2} - c_{\beta\alpha} \frac{3}{t_\beta} \right) + \lambda_7 v (-s_{\beta\alpha} + c_{\beta\alpha} t_\beta). \end{aligned} \tag{A2}$$

The triple Higgs coupling relevant for the potential SM-like Higgs decay $h \to AA$ is given by

$$\begin{aligned} C_{hAA} = {}& \lambda_1 v \left(c_{\beta\alpha} \frac{t_\beta^2 - 1}{t_\beta^3} - s_{\beta\alpha} \frac{2}{t_\beta^2} \right) + c_{\beta\alpha} \frac{M_h^2}{v} \frac{1-t_\beta^2}{t_\beta^3} + s_{\beta\alpha} \left(\frac{M_h^2}{v} \frac{2+t_\beta^2}{t_\beta^2} - 2\frac{M_A^2}{v} \right) \\ & + \frac{M_h^2 - M_H^2}{v} \left(c_{\beta\alpha} \frac{t_\beta^2 - 1}{t_\beta^3} + c_{\beta\alpha} s_{\beta\alpha}^2 \frac{1-6t_\beta^2+t_\beta^4}{t_\beta^3} - 2s_{\beta\alpha} + 4s_{\beta\alpha} c_{\beta\alpha}^2 \frac{t_\beta^2 - 1}{t_\beta^2} \right) \\ & + \lambda_6 v \left(c_{\beta\alpha} \frac{t_\beta^2 - 2}{t_\beta^2} - s_{\beta\alpha} \frac{3}{t_\beta} \right) + \lambda_7 v (c_{\beta\alpha} + s_{\beta\alpha} t_\beta). \end{aligned} \tag{A3}$$

Section III A shows the implication of these formulas for vanishing coupling $C_{hAA} = 0$, which is important for the numerical results in Secs. III C and IV.

In the following we present useful additional relations in terms of the invariant parameters of Ref. [35] and the Higgs basis parameters $\Lambda_{1\ldots7}$, which shed additional light on our numerical results. As in Sec. III A we restrict ourselves to the case $c_{\beta\alpha} = 0$. The triple Higgs couplings are then given by (see Ref. [35] and footnote 15 of Ref. [37])

$$C_{HH^+H^-} = -\lambda_U v = \Lambda_7 v, \tag{A4}$$

$$C_{HAA} = -\lambda_U v = \Lambda_7 v, \tag{A5}$$

$$\begin{aligned} C_{hAA} &= -\lambda_T v = (-\Lambda_3 - \Lambda_4 + \Lambda_5) v \\ &= -\Lambda_3 v + 2(M_{H^\pm}^2 - M_A^2)/v, \end{aligned} \tag{A6}$$

while several parameters can be related to Higgs masses as follows:

[5]Here we comment on Ref. [52], which appeared shortly after the present paper, and which claims that large a_μ is possible for large M_A in the case of CP violation. We point out that the large a_μ does not result from CP violation but from (extremely) large considered values of $t_\beta (\cot\beta)$. However these large $t_\beta (\cot\beta)$ values are excluded by either LHC or B-physics results and therefore are not considered in the present paper.

$$\lambda v^2 = \Lambda_1 v^2 = M_h^2, \tag{A7}$$

$$\lambda_A v^2 = (\Lambda_1 - \Lambda_5) v^2 = M_A^2 - M_H^2 + M_h^2, \tag{A8}$$

$$\lambda_F v^2 = (\Lambda_5 - \Lambda_4) v^2 = 2(M_{H^\pm}^2 - M_A^2), \tag{A9}$$

and $c_{\beta\alpha} = 0$ implies

$$\hat{\lambda} = -\Lambda_6 = 0. \tag{A10}$$

The previous results seem to indicate that the triple Higgs couplings of the heavy Higgs bosons(s), C_{HAA} and $C_{HH^+H^-}$, are independent of C_{hAA}, even in the case where $C_{hAA} = 0$. However, the couplings become correlated and their possible ranges become restricted once perturbativity and stability of the Higgs potential are taken into account. To see this, we quote one special case of a necessary stability condition derived in Ref. [53]. The requirement $V_4 > 0$ (see Appendix of that reference) for the case $\rho = 1$, $\cos\theta = -1$, $\sin\gamma = \cos\gamma = 1/\sqrt{2}$ leads to

$$(\Lambda_2 + 2\Lambda_3 - 4\Lambda_7) v^2 - 4M_{H^\pm}^2 + M_h^2 + 4M_H^2 > 0 \quad (\text{unconstrained } C_{hAA}), \tag{A11}$$

$$(\Lambda_2 - 4\Lambda_7) v^2 - 4M_A^2 + M_h^2 + 4M_H^2 > 0 \quad (C_{hAA} = 0). \tag{A12}$$

These formulas show that (up to mass corrections) Λ_7 and thus $C_{HH^+H^-}$ are limited from above either by $(\Lambda_2 + 2\Lambda_3)/4$ or by $\Lambda_2/4$. Together with the requirement of perturbativity, which limits quartic Higgs couplings to at most 4π, this is compatible with the maximum values for $C_{HH^+H^-}$ found in Sec. IV and Fig. 5, of around 1000 GeV for unconstrained C_{hAA} and around 400–600 GeV for $C_{hAA} = 0$.

[1] G. W. Bennett *et al.* (Muon $(g-2)$ Collaboration), Phys. Rev. D **73**, 072003 (2006).
[2] T. Aoyama, M. Hayakawa, T. Kinoshita, and M. Nio, Phys. Rev. Lett. **109**, 111808 (2012).
[3] C. Gnendiger, D. Stöckinger, and H. Stöckinger-Kim, Phys. Rev. D **88**, 053005 (2013).
[4] A. L. Kataev, Phys. Rev. D **86**, 013010 (2012).
[5] R. Lee, P. Marquard, A. V. Smirnov, V. A. Smirnov, and M. Steinhauser, J. High Energy Phys. 03 (2013) 162; A. Kurz, T. Liu, P. Marquard, and M. Steinhauser, Nucl. Phys. **B879**, 1 (2014); A. Kurz, T. Liu, P. Marquard, A. V. Smirnov, V. A. Smirnov, and M. Steinhauser, Phys. Rev. D **92**, 073019 (2015); **93**, 053017 (2016).
[6] M. Davier, A. Hoecker, B. Malaescu, and Z. Zhang, Eur. Phys. J. C **71**, 1515 (2011); **72**, 1874(E) (2012); Eur. Phys. J. C**77**, 827 (2017); .
[7] K. Hagiwara, R. Liao, A. D. Martin, D. Nomura, and T. Teubner, J. Phys. G **38**, 085003 (2011).
[8] K. Hagiwara, A. Keshavarzi, A. D. Martin, D. Nomura, and T. Teubner, Nucl. Part. Phys. Proc. **287–288**, 33 (2017).
[9] A. Keshavarzi and T. Teubner, talks at *g-2 theory initiative*, June 2017, Fermilab, and at "PhiPsi 2017," June 2017, Mainz.
[10] F. Jegerlehner, EPJ Web Conf. **166**, 00022 (2018).
[11] F. Jegerlehner and R. Szafron, Eur. Phys. J. C **71**, 1632 (2011).
[12] M. Benayoun, P. David, L. DelBuono, and F. Jegerlehner, Eur. Phys. J. C **73**, 2453 (2013); **75**, 613 (2015); arXiv:1605.04474.
[13] A. Kurz, T. Liu, P. Marquard, and M. Steinhauser, Phys. Lett. B **734**, 144 (2014).
[14] G. Colangelo, M. Hoferichter, A. Nyffeler, M. Passera, and P. Stoffer, Phys. Lett. B **735**, 90 (2014).
[15] G. Colangelo, M. Hoferichter, M. Procura, and P. Stoffer, J. High Energy Phys. 09 (2014) 091; G. Colangelo, M. Hoferichter, B. Kubis, M. Procura, and P. Stoffer, Phys. Lett. B **738**, 6 (2014); G. Colangelo, M. Hoferichter, M. Procura, and P. Stoffer, J. High Energy Phys. 09 (2015) 074; Phys. Rev. Lett. **118**, 232001 (2017); J. High Energy Phys. 04 (2017) 161.
[16] V. Pauk and M. Vanderhaeghen, Phys. Rev. D **90**, 113012 (2014).
[17] T. Blum, S. Chowdhury, M. Hayakawa, and T. Izubuchi, Phys. Rev. Lett. **114**, 012001 (2015); T. Blum, N. Christ, M. Hayakawa, T. Izubuchi, L. Jin, and C. Lehner, Phys. Rev. D **93**, 014503 (2016); T. Blum, N. Christ, M. Hayakawa, T. Izubuchi, L. Jin, C. Jung, and C. Lehner, Phys. Rev. Lett. **118**, 022005 (2017).
[18] M. Ablikim *et al.* (BESIII Collaboration), Phys. Lett. B **753**, 629 (2016).
[19] B. Chakraborty, C. T. H. Davies, J. Koponen, G. P. Lepage, M. J. Peardon, and S. M. Ryan, Phys. Rev. D **93**, 074509 (2016).
[20] R. M. Carey, K. R. Lynch, J. P. Miller, B. L. Roberts, W. M. Morse, Y. K. Semertzides, V. P. Druzhinin, B. I. Khazin *et al.*, Report No. FERMILAB-PROPOSAL-0989, http://lss.fnal.gov/archive/test-proposal/0000/fermilab-proposal-0989.pdf; B. L. Roberts, Chin. Phys. C **34**, 741 (2010).
[21] H. Iinuma (J-PARC New $g-2$/EDM Experiment Collaboration), J. Phys. Conf. Ser. **295**, 012032 (2011).
[22] A. Broggio, E. J. Chun, M. Passera, K. M. Patel, and S. K. Vempati, J. High Energy Phys. 11 (2014) 058.
[23] E. J. Chun and J. Kim, J. High Energy Phys. 07 (2016) 110.
[24] L. Wang and X. F. Han, J. High Energy Phys. 05 (2015) 039.
[25] T. Abe, R. Sato, and K. Yagyu, J. High Energy Phys. 07 (2015) 064.
[26] A. Crivellin, J. Heeck, and P. Stoffer, Phys. Rev. Lett. **116**, 081801 (2016).

[27] E. J. Chun, Z. Kang, M. Takeuchi, and Y. L. S. Tsai, J. High Energy Phys. 11 (2015) 099.
[28] T. Han, S. K. Kang, and J. Sayre, J. High Energy Phys. 02 (2016) 097.
[29] V. Ilisie, J. High Energy Phys. 04 (2015) 077.
[30] A. Cherchiglia, P. Kneschke, D. Stöckinger, and H. Stöckinger-Kim, J. High Energy Phys. 01 (2017) 007.
[31] A. Pich and P. Tuzon, Phys. Rev. D **80**, 091702 (2009).
[32] M. Jung, A. Pich, and P. Tuzon, J. High Energy Phys. 11 (2010) 003.
[33] T. Abe, R. Sato, and K. Yagyu, J. High Energy Phys. 07 (2017) 012.
[34] S. M. Barr and A. Zee, Phys. Rev. Lett. **65**, 21 (1990); **65**, 2920 (1990).
[35] J. F. Gunion and H. E. Haber, Phys. Rev. D **67**, 075019 (2003).
[36] G. C. Branco, P. M. Ferreira, L. Lavoura, M. N. Rebelo, M. Sher, and J. P. Silva, Phys. Rep. **516**, 1 (2012).
[37] S. Davidson and H. E. Haber, Phys. Rev. D **72**, 035004 (2005); **72**, 099902(E) (2005).
[38] M. Misiak and M. Steinhauser, Eur. Phys. J. C **77**, 201 (2017).
[39] S. Gori, H. E. Haber, and E. Santos, J. High Energy Phys. 06 (2017) 110.
[40] D. Eriksson, J. Rathsman, and O. Stal, Comput. Phys. Commun. **181**, 189 (2010); **181**, 833 (2010).
[41] P. Bechtle, O. Brein, S. Heinemeyer, G. Weiglein, and K. E. Williams, Comput. Phys. Commun. **181**, 138 (2010); **182**, 2605 (2011); P. Bechtle, O. Brein, S. Heinemeyer, O. Stål, T. Stefaniak, G. Weiglein, and K. E. Williams, Eur. Phys. J. C **74**, 2693 (2014).
[42] P. Bechtle, S. Heinemeyer, O. Stål, T. Stefaniak, and G. Weiglein, Eur. Phys. J. C **74**, 2711 (2014).
[43] C. Patrignani *et al.* (Particle Data Group), Chin. Phys. C **40**, 100001 (2016).
[44] A. M. Sirunyan *et al.* (CMS Collaboration), Phys. Lett. B **779**, 283 (2018).
[45] M. Aaboud *et al.* (ATLAS Collaboration), Phys. Rev. Lett. **119**, 051802 (2017).
[46] J. Abdallah *et al.* (DELPHI Collaboration), Eur. Phys. J. C **38**, 1 (2004).
[47] X. Q. Li, J. Lu, and A. Pich, J. High Energy Phys. 06 (2014) 022.
[48] T. Enomoto and R. Watanabe, J. High Energy Phys. 05 (2016) 002.
[49] P. Arnan, D. Bečirević, F. Mescia, and O. Sumensari, Eur. Phys. J. C **77**, 796 (2017).
[50] CMS Collaboration, Search for additional neutral Higgs bosons decaying to a pair of tau leptons in pp collisions at *pp* collisions at = $\sqrt{s} = 7$ and 8 TeV, CMS Physics Analysis Summary Report No. CMS-PAS-HIG-14-029, CERN, 2014, https://cds.cern.ch/record/2041463/les/HIG-14-029-pas.pdf.
[51] S. Hessenberger and W. Hollik, Eur. Phys. J. C **77**, 178 (2017).
[52] V. Keus, N. Koivunen, and K. Tuominen, arXiv:1712.09613.
[53] A. W. El Kaffas, W. Khater, O. M. Ogreid, and P. Osland, Nucl. Phys. **B775**, 45 (2007).